Joint Int. Conf. on Math. Methods and Supercomp. in Nuc. Appl., April 19-23, 1993, Karlsruhe, Germany,
Proc. Ed. H. Küsters, E. Stein, W. Werner, Kernforschungszentrum Karlsruhe, 1993, Vol.1, pp. 224 - 235

CONTRIBUTIONS TO TURBULENCE MODELLING OF NATURAL CONVECTION IN LIQUID METALS BY DIRECT NUMERICAL SIMULATION

M. Wörner, G. Grötzbach
Kernforschungszentrum Karlsruhe
Institut für Reaktorsicherheit
Postfach 3640, D-7500 Karlsruhe
Germany
Tel. 07247/822577

ABSTRACT

Direct numerical simulations are performed for turbulent Rayleigh-Bénard convection in liquid sodium and air at similar Grashof numbers. Results are achieved by the finite volume code TURBIT, which was extended by a semi-implicit time integration scheme for the thermal energy equation to improve considerably the computational efficiency for liquid metal convection. Spectral analysis of the numerical results shows the similarity of small scale structures in the velocity field of both fluids, whereas the temperature fields are completely different. Terms in the transport equations of turbulent kinetic energy and turbulent heat flux are evaluated from the numerical results, using analytical definitions. It is found that for liquid metals model assumptions for turbulence terms dominated by small scales of the velocity field do not need, terms influenced by the temperature field but very well need adaptation to the influence of molecular Prandtl number. In liquid metal convection molecular thermal transport phenomena are of great importance. The diffusive transport of turbulent heat flux in natural convection is mainly due to the action of pressure fluctuations and not, as usually assumed, due to velocity fluctuations. The conventional model assumption for closure of turbulent diffusion is analysed.

INTRODUCTION

In new fast breeder designs great efforts are made to take advantage of inherent safety features. For example it is aimed that decay heat can be removed completely by natural convection[1]. In this context experiments are performed in scaled reactor models using water as a model fluid[2]. The interpretation of the experiments and the transfer of the results to reactor conditions, where liquid sodium is used as coolant, is mainly done by computer codes [3,4]. Turbulence models used in these codes are being improved to be applicable to purely buoyant flows, especially in liquid metals[5]. Thus detailed turbulence data of such flows are required to calibrate turbulence models and to improve model assumptions for this special application. Due to difficulties in working with liquid metals only very few experimental data

suitable for model validation are available. Here we use the method of direct numerical simulation of turbulence to provide such data for at least small turbulence levels.

In this paper we give an introduction to the simulation method and the computer code TURBIT[6]. We discuss special features of liquid metals and the consequences for an efficient numerical scheme, as there is the need for semi-implicit time integration of the thermal energy equation. Physically we consider the Rayleigh-Bénard convection, that is the convection in an infinite horizontal fluid layer heated at the lower and cooled at the upper wall. We use results of our numerical simulations to analyse statistical features of turbulence in liquid sodium and air, whereas in a second paper[7] we focus on macroscopic mechanisms and structures of the flow. In continuing a previous study[8] where we looked at the concept of turbulent Prandtl number for modelling the turbulent heat flux we now analyse terms of the transport equation of turbulent heat flux. Finally conclusions will be drawn on which further developments one should focus on to adapt existing turbulence models for application to natural convection in liquid metals.

SIMULATION METHOD

The method of direct numerical simulation of turbulence is based on the full conservation equations of mass, momentum and thermal energy. The features of turbulence require to solve these equations in three dimensions and in time, and to use grids which resolve the largest and smallest scales of turbulence. Here these requirements are met. Therefore no assumptions for the subgrid scales and no wall models are needed and the simulations do not depend on any model coefficients.

The computer code TURBIT is based on a finite volume method and allows for direct and large eddy simulation of turbulent flow in simple channel geometries[6]. The basic equations are solved on a staggered grid in a dimensionless form. For normalisation the channel height D, velocity $u_0 = (g\ \beta\ \Delta T_w\ D)^{1/2}$, time D/u_0 and temperature difference ΔT_w are used, where g = gravity, β = volume expansion coefficient, ΔT_w = temperature difference between the two walls. The Boussinesq-approximation is assumed to be valid. Spatial discretisation is done by second order central finite differences. For time integration of the momentum and thermal energy equation the explicit Euler-Leapfrog scheme is used.

IMPROVEMENT OF TIME-INTEGRATION

Liquid metals are characterised by very low values of the molecular Prandtl-number $Pr = \nu/\kappa$, that is the ratio of kinematic and thermal diffusivity. Due to the high thermal conductivity of liquid metals small-scaled disturbances in the temperature field are compensated rapidly. Thus the thermal diffusion process is highly efficient and involves a very small time scale. A fully explicit time integration scheme has to resolve this time scale for reasons of numerical stability and thus allows for the use of very small time steps only. Since these time steps are much smaller than those required to resolve even the highest frequencies of turbulence fully explicit time integration schemes are very inefficient for numerical simulation of liquid metal flows. Much larger time steps can be used if the diffusive terms in the thermal energy equation are treated implicitly. Therefore we implemented

in TURBIT two semi-implicit time integration schemes, the Leapfrog Crank-Nicolson and the Adams-Bashforth Crank-Nicolson scheme respectively[9]. Both can be used alternatively and allow for an increase of the time step up to a factor of 50 compared to the fully explicit Euler-Leapfrog scheme, which is still used for the momentum equations. It is important to note that this increase of the time step does not involve any loss of physically relevant information of turbulence.

In implicit or semi-implicit time integration schemes a set of linear equations has to be solved which implies an additional computational effort compared to explicit schemes. This set of equations has to be solved efficiently to achieve a remarkable reduction of the computational costs. The resulting set of equations of our semi-implicit time integration schemes is very similar to that of a discretised Poisson equation, since the diffusive term contains the Laplace operator. In TURBIT we use the projection method of Chorin and have to solve a Poisson equation with Neumann boundary conditions at walls for the pressure at every time step to fulfil the conservation of mass. We use a vectorized direct solver based on the fast Fourier transform and Gaussian elimination[10]. This solver has been modified to allow for the solution of the set of linear equations and for Neumann and Dirichlet boundary conditions for the temperature. With this solver the additional CPU-time per time step of the semi-implicit scheme compared to the explicit one is only 10 to 20 percent. Therefore the effective gain in total CPU-time of a simulation with the semi-implicit scheme achieves up to a factor of 40, depending on grid and Prandtl-number. For verification of the new simulation method we successfully recalculated a benchmark of 2D convection of a low Prandtl-number fluid in a rectangular box[9].

CASE SPECIFICATIONS

The Rayleigh-Bénard problem is characterised by two dimensionless numbers, the Rayleigh-number $Ra = g \beta \Delta T_w D^3/(\nu\kappa)$ and the Prandtl-number mentioned above. From both a further dimensionless number, the Grashof-number $Gr = Ra/Pr$, can be defined. Here we consider three simulations (see Table 1), two of liquid sodium ($Pr = 0.006$) and one of air ($Pr = 0.71$). Although Ra and Pr are clearly different in the sodium and air cases, the Grashof numbers are of the same magnitude.

Grids used in direct numerical simulation have to meet several requirements to ensure physical relevance of the results. The grid widths Δx_i ($i = 1,2$ horizontal, $i = 3$ vertical) have to be fine enough to resolve the smallest scales of turbulence and Δx_{3wall} to resolve the thin boundary layers. The extensions $X_{1,2}$ of the control volume in the horizontal directions, where periodic boundary conditions are used, have to be large enough to allow for development of large scale structures. The numbers of mesh cells N_i follow directly from the values chosen for X_i and Δx_i, except for the vertical direction in which non-equidistant grids are used. For simulations with air sufficient experience is available to specify adequate grids[11]. In contrast, a sensitivity study was necessary for liquid sodium to investigate the influence of Δx_i and X_i on the numerical results [8].

The simulation for $Ra = 6{,}000$ was started from zero velocities and a linear mean temperature profile on which random fluctuations were superimposed. To reduce the computational costs, the long transient from fluid at rest to fully developed flow was run on a coarser grid. The final 3D results were interpolated to the finer mesh and the simulation continued. Nevertheless, the total CPU-time on the

Fujitsu VP400 at the Nuclear Research Centre Karlsruhe for this run was about 60 hours. The simulation for sodium, Ra = 24,000, was started from the final data of a previous simulation (Ra = 12,000, Pr = 0.006) run on the same grid. For the simulation of air final results of a former air-simulation at Ra = 380,000 were interpolated and used as initial data.

SIMULATION RESULTS

VERIFICATION

For verification of the simulation with air we use results of an experiment performed by Deardorff [12] for the same Rayleigh-number. Vertical profiles of mean temperature and rms-values of the vertical velocity are given in Fig. 1. For reasons of symmetry only the lower half of the channel ($x_3 = 0$: lower wall, $x_3 = 1$: upper wall) is shown. The numerical results agree well with the experimental ones except for $u_{3\,rms}$ near the wall. This discrepancy may be a consequence of inaccurate measurements. This can be supposed due to the unsystematic correlation coefficient between temperature and u_3 near the walls given in reference 12.

For Rayleigh-Bénard convection in liquid sodium there are only very few experimental data available which can be used for verification. The calculated Nusselt-numbers compare roughly with the experiments of Kek[13], see Table 2. The small values of Nu show that most heat is transferred by conduction, not by convection. Significantly better agreement is achieved for the rms-value of temperature fluctuations in channel midwidth. The results given in Table 2 in terms of the wall temperature difference agree well with the band of experimental data given by Kek[13].

GRASHOF-ANALOGY

In Fig. 2 we compare power spectra of spatial fluctuations of vertical velocity and temperature in channel midheight for the simulation of air ($Gr = 8.9 \cdot 10^5$) and liquid sodium ($Gr = 10^6$). Especially for velocity fluctuations of high frequencies (wavenumbers $\log(k_1) > 1$) we find nearly identical power spectra. Obviously there is a scaling of the velocity field with the Grashof number. Differences can be seen in the left part of the spectrum, which corresponds to large spatial structures. This is due to the different features of the temperature field in liquid sodium and air (see Fig. 2) and its influence on the velocity field by buoyancy forces. In air the temperature and velocity fields are very similar, according to the Prandtl number being near unity. In liquid sodium turbulence features of the temperature field are clearly different to that of the velocity field, since the high thermal diffusivity allows only for lowfrequent temperature fluctuations (see computer generated movie to be presented at this conference[7]).

BALANCE EQUATION OF TURBULENT KINETIC ENERGY

Standard k-ε turbulence models[14] use the eddy diffusivity hypothesis and solve transport equations for the turbulent kinetic energy $k = \overline{u_i'^2}/2$ and its dissipation rate ε to close the time averaged Navier-Stokes equations. In turbulent Rayleigh-

Bénard convection considered here, there exists no mean flow. Therefore the transport equation of k reduces to a form where no convective transport and no production of k by shear stresses and mean velocity gradients is present. The balance of k is dominated only by production/destruction G due to buoyancy effects, by the diffusion D and the dissipation ε:

$$\frac{\partial k}{\partial t} = \underbrace{\overline{u_3' T'}}_{G} \underbrace{- \frac{\partial}{\partial x_3} \left(\overline{u_3' k} + \overline{u_3' p'} - \frac{1}{\sqrt{Gr}} \frac{\partial k}{\partial x_3} \right)}_{D} - \varepsilon. \qquad (1)$$

In Fig. 3 we present results for these terms, which were analysed using their analytical definition, for the simulation of liquid sodium (Gr = 10^6) and air. The vertical profile of the dissipation ε is very similar for both simulations. This is evident, because the dissipation is mainly caused by highfrequent velocity fluctuations. As discussed above, these scale with the Grashof number (see Fig. 2) which is of the same magnitude for both simulations. The vertical profile of the production term G is clearly different for both fluids, as one would expect by the totally different temperature spectra. The remaining balance term is the diffusive transport D. It redistributes turbulent kinetic energy produced by G. Here we consider fully developed flow. Therefore the differences in the vertical profiles of D are just consequences of the similar ε and different G profiles, though D is evaluated separately.

Fig. 3 indicates that in natural convection the assumption of local equilibrium, that means a local balance between production and dissipation of k, is not valid. This observation is in agreement with results for the natural convection boundary layer at a heated vertical plate[15]. Besides, Fig. 3 shows that for turbulence modelling in liquid metals model assumptions for turbulence terms dominated by small scales of the velocity field, like the dissipation terms, are not expected to need special adaptation to the influence of molecular Prandtl number because the Grashof analogy may be used. On the other hand terms dominated by the large scales and influenced by the temperature field strongly depend on Pr and Ra.

BALANCE EQUATION OF TURBULENT HEAT FLUX

In standard k-ε models the turbulent heat flux $\overline{u_3'T'}$ is modelled on the basis of an eddy diffusivity of heat κ_t. Usually the concept of turbulent Prandtl-number $Pr_t = \nu_t/\kappa_t$ is used to calculate κ_t from the eddy diffusivity of mass and from the empirically established coefficient Pr_t. This concept gives only poor results for natural convection and especially for liquid metals because it simply transfers features of turbulence from the velocity to the temperature field[8]. For liquid metals, however, turbulence features of temperature and velocity field are clearly different (see Fig. 2).

More promising concepts than that of using a turbulent Prandtl-number are based on the transport equation for the turbulent heat flux. For Rayleigh-Bénard convection the transport equation for $\overline{u_3'T'}$ reduces to

$$\frac{\partial \overline{u_3'T'}}{\partial t} = \underbrace{-\frac{\partial}{\partial x_3}\left(\overline{u_3'^2T'} + \overline{p'T'} - \frac{1}{Pr\sqrt{Gr}}\overline{u_3'\frac{\partial T'}{\partial x_3}} - \frac{1}{\sqrt{Gr}}\overline{T'\frac{\partial u_3'}{\partial x_3}}\right)}_{D} \tag{2}$$

$$\underbrace{-\overline{u_3'^2}\frac{\partial \overline{T}}{\partial x_3} + \overline{T'^2}}_{P} \quad \underbrace{-\frac{1}{\sqrt{Gr}}\left(1+\frac{1}{Pr}\right)\overline{\frac{\partial u_3'}{\partial x_i}\cdot\frac{\partial T'}{\partial x_i}}}_{MD} \quad \underbrace{+\overline{p'\frac{\partial T'}{\partial x_3}}}_{PS}$$

Here D denotes the diffusion of $\overline{u_3'T'}$, consisting of a turbulent part (first two terms) and a molecular part (last two terms). Responsible for the production of $\overline{u_3'T'}$ are both the mean temperature field (first part of P) and the buoyancy force (second part of P). The molecular destruction MD vanishes only for isotropic turbulence. In this case the pressure scrambling term PS is the only dissipation term[16].

Direct comparison of the balance of turbulent heat flux between air and sodium simulations is not meaningful, since the vertical profiles of $\overline{u_3'T'}$ are clearly different for both fluids (see production terms $G = \overline{u_3'T'}$ in Fig. 3). In the following we concentrate on sodium case Ra = 24,000. The vertical profiles of the different terms, given in Fig. 4, show, that not the pressure scrambling term but the molecular destruction is the main sink of turbulent heat flux. In the corresponding balance of the simulation with air (not shown here) the molecular destruction is of minor importance, as compared to the pressure scrambling term. However, it is not zero because the flow is not isotropic. For liquid metals it is the dominance of thermal diffusion in the temperature field, that causes the molecular destruction to play such an important role for this type of fluid. The production term P is zero at the walls and increases towards the centre of the channel. Here we find a surplus of P over the molecular destruction and pressure scrambling term. This surplus is balanced by the diffusion D which redistributes turbulent heat flux from the centre of the channel to the near wall regions.

Terms that have to be modelled to close the transport equation for the turbulent heat flux are the diffusion and the pressure scrambling term. Here we consider only closure assumptions for diffusive transport. Usually molecular diffusion and diffusion by pressure fluctuations are neglected[17]. Therefore only the correlation $\overline{u_3'^2T'}$ has to be modelled. In Fig. 5 we compare vertical profiles of $\overline{u_3'^2T'}$ and $\overline{p'T'}$ and find, that in Rayleigh-Bénard convection turbulent diffusion is mainly caused by pressure fluctuations. Thus $\overline{p'T'}$ seems to be an important term that must be modelled adequately.

The model commonly used for closure of turbulent diffusion is[16]

$$- \overline{u_3'^2 T'} = 2\, c_T \frac{k}{\varepsilon} \overline{u_3'^2} \frac{\partial \overline{u_3' T'}}{\partial x_3}, \qquad (3)$$

where C_T is approximately 0.1. In Fig. 6 we show the vertical profile of C_T evaluated from our numerical results. Additionally the vertical profile of

$$C_{TS} = \frac{- \left(\overline{u_3'^2 T'} + \overline{p' T'} \right)}{2 \frac{k}{\varepsilon} \overline{u_3'^2} \frac{\partial \overline{u_3' T'}}{\partial x_3}} \qquad (4)$$

is given, which implies that both, turbulent diffusion by velocity and pressure fluctuations, are modelled in common by the right hand side of Equation (3). It can be seen that both, C_T and C_{TS} are almost constant through the channel. Only near the walls a strong increase is observed. The small peaks found in Fig. 6 at channel midwidth can be explained by the vanishing gradient of turbulent heat flux, appearing in the denominator. In general, the model assumption given above seems to be a reasonable approximation for turbulent diffusion as additional wall corrections are used. However, the values $C_T \approx 0.008$ and $C_{TS} \approx 0.02$ resulting from the analysis are about a magnitude lower than the ones commonly used. Furthermore, the gradient diffusion concept may in principle be inadequate because it implies that in case of constant turbulent heat flux there can be no diffusion. Results for the simulation with air reveal, however, that in the centre of the channel there is a diffusive transport, though the turbulent heat flux is constant in this region.

CONCLUSIONS

The method of direct numerical simulation was used to produce a data base for Rayleigh-Bénard convection in air and liquid sodium at small turbulence levels. While the molecular Prandtl-number and Rayleigh-number are clearly different in the simulations with air and sodium the Grashof-numbers are of same magnitude. The results are used to analyse spectral features of turbulence in both fluids. It is found that small scale structures of the velocity field scale with the Grashof number. Differences at large scale structures can be attributed to the totally different temperature fields in both fluids, which act on the velocity field by buoyancy forces.

For both fluids terms of the transport equation of turbulent kinetic energy were calculated from the simulation data. Terms dominated by small scales of the velocity field, like the dissipation ε, are found to be very similar in both fluids. This is in accordance to the Grashof analogy of the velocity field. However, clearly

different behaviour is observed for all terms influenced by the temperature field. We conclude that model assumptions for such terms need special adaptation to the influence of molecular Prandtl number to be applicable to liquid metal convection.

This conclusion especially concerns the modelling of turbulent heat flux. For liquid sodium an analysis of terms of the transport equation of turbulent heat flux was performed. The results reveal the molecular destruction to be the main sink of turbulent heat flux in liquid metal convection. In turbulence models based on the transport equation of turbulent heat flux this term is usually neglected because isotropic turbulence is assumed. However, in liquid metal convection turbulence is far away from being locally isotropic. The diffusive transport of turbulent heat flux is also found to be of great importance. It is responsible for redistribution of turbulent heat flux from the centre of the channel to the near wall regions. In natural convection turbulent diffusion is mainly due to the action of pressure fluctuations, not due to velocity fluctuations. However, the opposite is true for forced convection. Therefore turbulence models usually neglect pressure diffusion and account only for diffusion by velocity fluctuations. Analysis of the conventional model assumption yields reliable results, with exception of the near wall regions. Nevertheless, for natural convection adequate modelling of pressure diffusion is essential.

In future work we will concentrate on analysis of model assumptions of further closure terms in the transport equation of turbulent heat flux as there are molecular diffusion and pressure scrambling terms.

ACKNOWLEDGEMENT

The methods for analysis of the transport equation of turbulent heat flux were provided by I. Hiltner and Ch. Seiter. Their work is gratefully acknowledged.

REFERENCES

1 K. Satoh, H. Miyakoshi, "Study of decay heat removal by natural circulation," Proc. NURETH-4, (1989), pp. 378-383.

2 H. Hoffmann, H. Kamide, K. Marten, H. Ohshima, D. Weinberg, "Investigations on the transition from forced to natural convection for the pool type EFR in the 3d RAMONA model," Int. Conf. on Fast Reactors and Related Fuel Cycles, Oct. 28 - Nov. 1, 1991, Kyoto.

3 H. Ninokata, "Advances in computer simulation of fast breeder reactor thermalhydraulics," Proc. SNA '90, (1990), pp.80-85.

4 H.A. Borgwaldt, "CRESOR, a robust vectorized Poisson solver implemented in the COMMIX-2(V) thermal-hydraulics code," Proc. SNA '90, (1990), pp. 346-351.

5 S.P. Lawrence, "Turbulence modelling in naturally convecting fluids," Culham Lab., CLM-R292, Sept. 1989.

6 G. Grötzbach, "Direct numerical and large eddy simulation of turbulent channel flows," Encyclopaedia of Fluid Mechanics, Gulf Publ. Houston, Vol. 6, (1987), pp. 1337-1391.

7 G. Grötzbach, M. Wörner, "Analysis of flow mechanisms in Rayleigh-Bénard convection at small Prandtl numbers," This conference.

8 G. Grötzbach, M. Wörner, "Analysis of second order transport equations by numerical simulations of turbulent convection in liquid metals," Proc. NURETH-5, (1992), pp. 358-365.

9 M. Wörner, G. Grötzbach, "Analysis of semi-implicit time integration schemes for direct numerical simulation of turbulent convection in liquid metals," in: Notes on Numerical Fluid Mechanics, Vol. 35, Ed. J.B. Vos, A. Rizzi, I.L. Ryhming, Vieweg Verlag Braunschweig (1992), pp. 542-551.

10 H. Schmidt, U. Schumann, H. Volkert, W. Ulrich, "Three-dimensional, direct and vectorized elliptic solvers for various boundary conditions," DFVLR-Mitteilung 84-15, (1984).

11 G. Grötzbach, "Spatial resolution requirements for direct num. simulation of the Rayleigh-Bénard convection," J. Comp. Phys. 49, (1983), pp. 241-264.

12 J.W. Deardorff, G.E. Willis, "Investigation of turbulent thermal convection between horizontal planes," J. Fluid Mech., Vol. 28, (1967), pp. 576-704.

13 V. Kek, "Bénard Konvektion in flüssigen Natriumschichten," Dr.-thesis, Universität Karlsruhe, KfK 4611, (1989).

14 W. Rodi, "Turbulence models and their application in hydraulics - a state of the art review ," IAHR-publication, Delft 1980.

15 T.W.J. Peeters, R.A.W.M. Henkes, "The Reynolds-stress model of turbulence applied to the natural-convection boundary layer along a heated vertical plate," Int. J. Heat Mass Transfer, Vol. 35, (1992), pp. 403-420.

16 M.S. Hossain, W. Rodi, "A turbulence model for buoyant flows and its application to vertical buoyant jets," in Turbulent jets and plumes; Ed. W. Rodi, Pergamon Press (1982).

17 B.E. Launder, "Heat and Mass Transport," in Topics in Applied Physics, Vol. 12, Ed. P. Bradshaw, Springer (1976).

Table 1. Parameter and grid data of the simulations

Pr	Ra	Gr	$X_{1,2}$	$\Delta x_{1,2}$	Δx_{3w}	$N_{1,2}$	N_3
0.006	6,000	10^6	8.0	0.04	0.01	200	31
0.006	24,000	$4 \cdot 10^6$	8.0	0.032	0.005	250	39
0.71	630,000	$8.9 \cdot 10^5$	7.92	0.0396	0.005	200	39

Table 2. Verification of sodium simulations

Ra	Nusselt-number TURBIT	Nusselt-number experiment[13]	T_{rms} TURBIT	T_{rms} experiment[13]
6,000	1.04	1.10	6.3	6.5 ± 1.5
24,000	1.37	1.49	17.0	16.0 ± 3.0

Fig. 1: Mean temperature profile and rms-value of vertical velocity in air: —— TURBIT, ● experiment[12]. (Overbar denotes ensemble / time averaging, prime denotes the fluctuating part of variable).

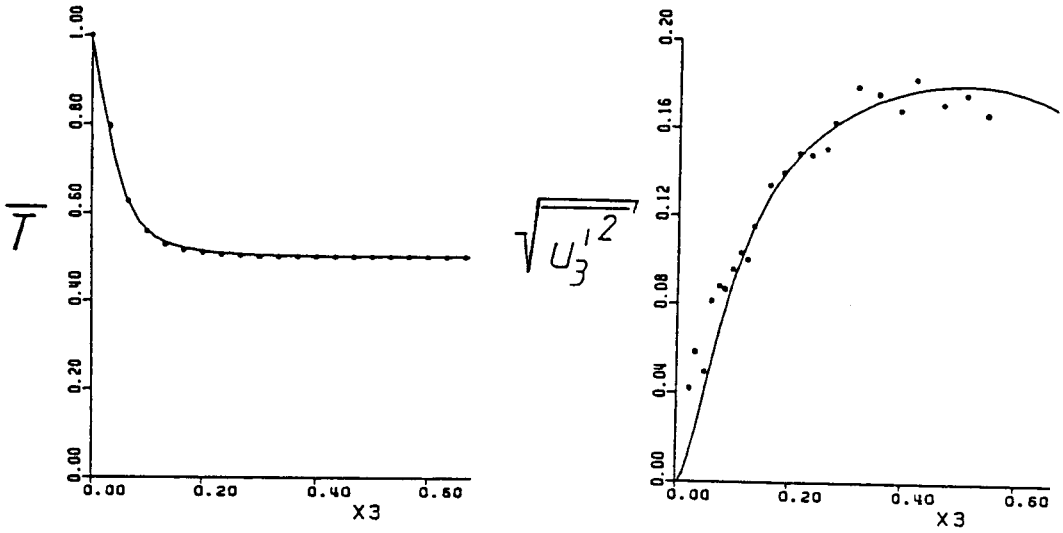

Fig. 2: Powerspectra of temperature fluctuations (left) and vertical velocity (right) in channel-midwidth: o air, Δ liquid sodium (Ra = 6,000).

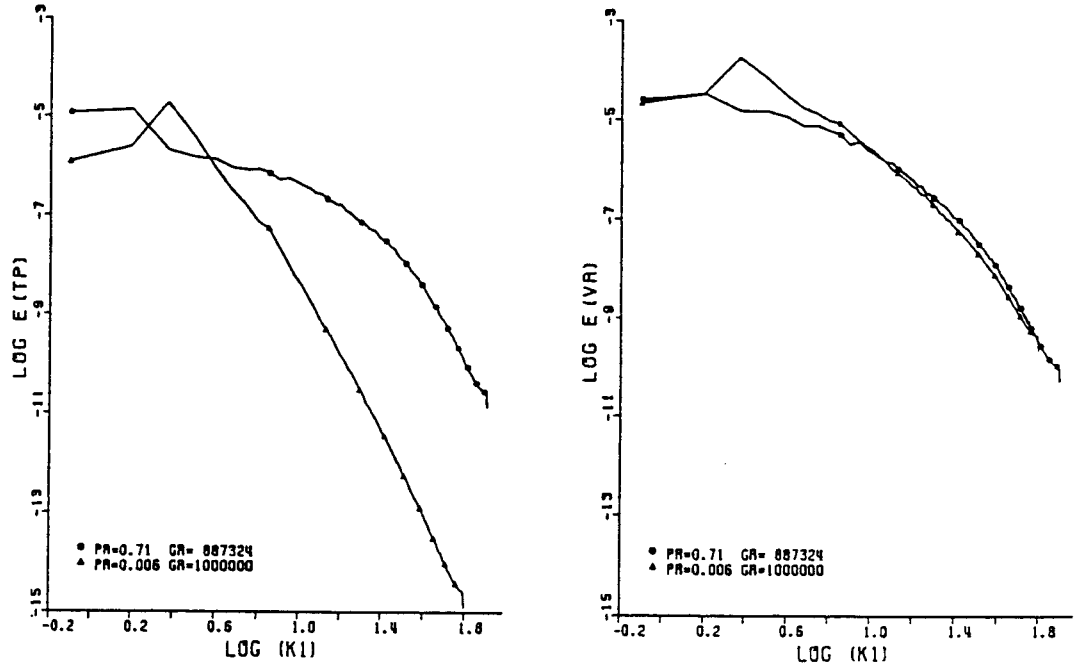

Fig. 3: Terms of the k-equation for air (left) and liquid sodium (Ra = 6,000, right): □ production, Δ diffusion, o dissipation.

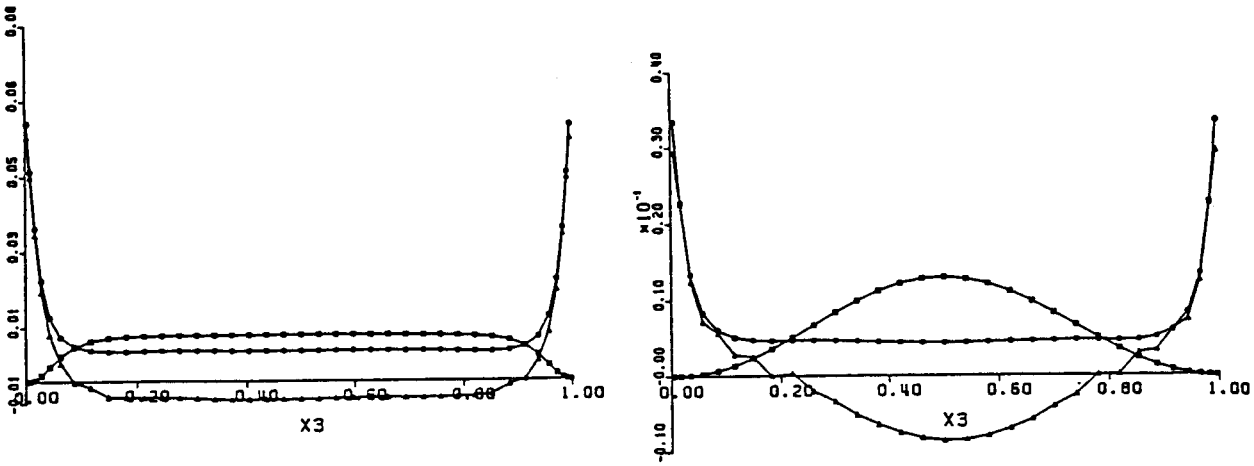

Fig. 4: Terms of the $\overline{u_3'T'}$ - equation in liquid sodium (Ra = 24,000): □ diffusion, o production, Δ molecular destruction, + pressure scrambling term.

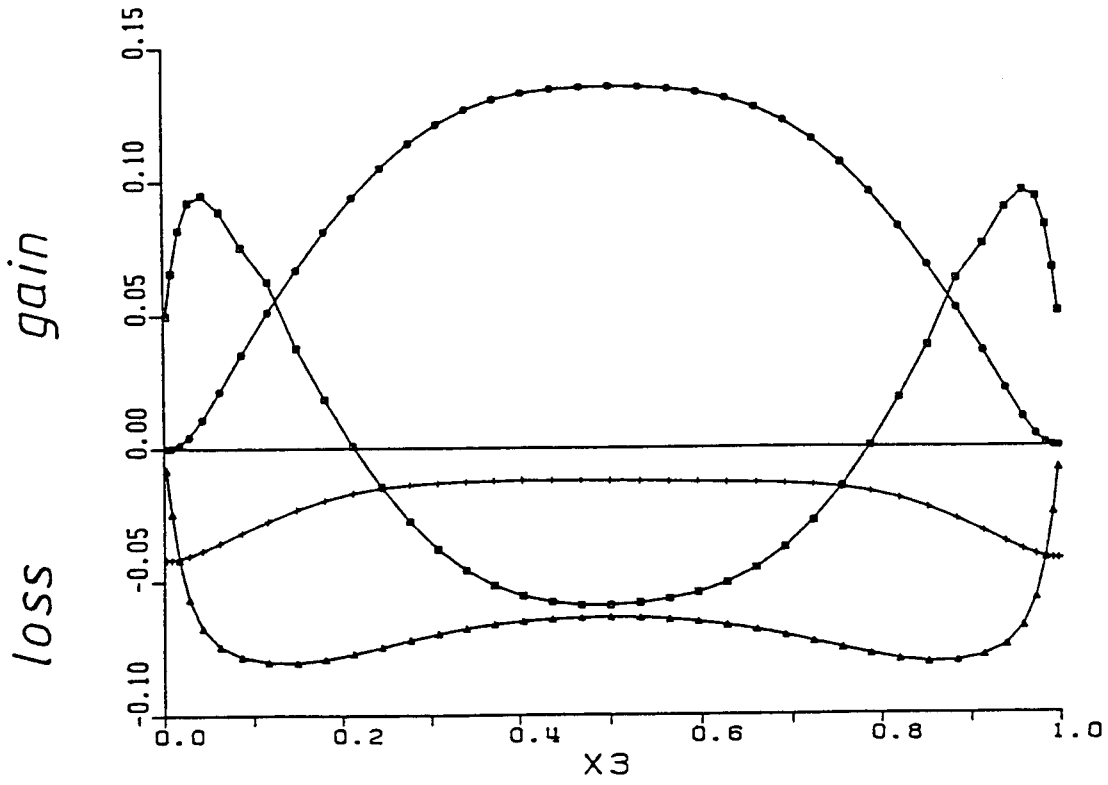

Fig. 5: Turbulent diffusion terms in liquid sodium (Ra = 24,000): □ $\overline{p'T'}$, Δ $\overline{u_3'^2T'}$.

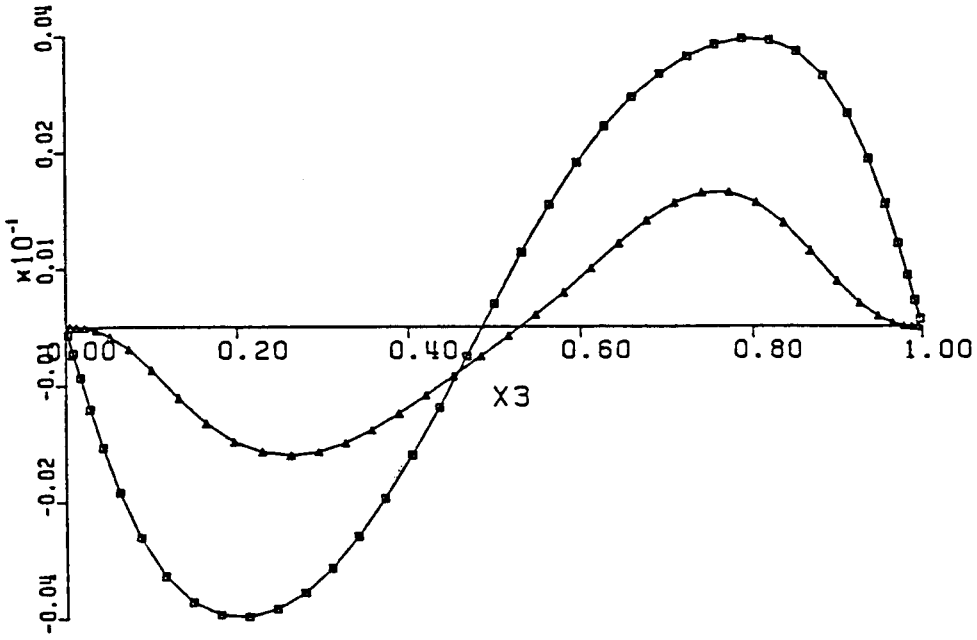

Fig. 6: Coefficients of turbulent diffusion model of $\overline{u_3'T'}$: □ C_T, Δ C_{TS}.